

Selective blood-brain barrier permeabilization of brain metastases by a type 1 receptor-selective tumor necrosis factor mutein

Mario F. Munoz Pinto, Sandra J. Campbell, Christina Simoglou Karali, Vanessa A. Johanssen, Claire Bristow, Vinton W. T. Cheng, Niloufar Zarghami, James R. Larkin, Maria Pannell, Arron Hearn, Cherry Chui, Barbara Brinquis Nunez, Evert Bokma, Robert Holgate, Daniel C. Anthony, and Nicola R. Sibson

Medical Research Council Institute for Radiation Oncology, Department of Oncology, University of Oxford, Oxford, UK (M.F.M.P., S.J.C., C.S.K., V.A.J., C.B., V.W.T.C., N.Z., J.R.L., M.P., N.R.S.); Abzena Ltd., Babraham Research Campus, Babraham, Cambridge, UK (A.H., C.C., B.B.N., E.B., R.H.); Department of Pharmacology, University of Oxford, Oxford, UK (D.C.A.)

Present affiliations: Center for Neuroscience and Cell Biology (CNC), University of Coimbra, Coimbra, Portugal (MFMP); MRC Weatherall Institute of Molecular Medicine, University of Oxford, John Radcliffe Hospital, Oxford, UK (CSK); Leeds Institute of Medical Research, University of Leeds, Leeds, UK (VWTC); OxSonic Ltd., The Magdalen Centre, Oxford Science Park, Oxford, UK (MP)

Corresponding Author: Nicola R. Sibson, PhD, Department of Oncology, University of Oxford, Old Road Campus Research Building, Oxford OX3 7DQ, UK (nicola.sibson@oncology.ox.ac.uk).

Abstract

Background. Metastasis to the brain is a major challenge with poor prognosis. The blood-brain barrier (BBB) is a significant impediment to effective treatment, being intact during the early stages of tumor development and heterogeneously permeable at later stages. Intravenous injection of tumor necrosis factor (TNF) selectively induces BBB permeabilization at sites of brain micrometastasis, in a TNF type 1 receptor (TNFR1)-dependent manner. Here, to enable clinical translation, we have developed a TNFR1-selective agonist variant of human TNF that induces BBB permeabilization, while minimizing potential toxicity.

Methods. A library of human TNF muteins (mutTNF) was generated and assessed for binding specificity to mouse and human TNFR1/2, endothelial permeabilizing activity in vitro, potential immunogenicity, and circulatory half-life. The permeabilizing ability of the most promising variant was assessed in vivo in a model of brain metastasis.

Results. The primary mutTNF variant showed similar affinity for human TNFR1 than wild-type human TNF, similar affinity for mouse TNFR1 as wild-type mouse TNF, undetectable binding to human/mouse TNFR2, low potential immunogenicity, and permeabilization of an endothelial monolayer. Circulatory half-life was similar to mouse/human TNF and BBB permeabilization was induced selectively at sites of micrometastases in vivo, with a time window of ≥ 24 hours and enabling delivery of agents within a therapeutically relevant range (0.5–150 kDa), including the clinically approved therapy, trastuzumab.

Conclusions. We have developed a clinically translatable mutTNF that selectively opens the BBB at micrometastatic sites, while leaving the rest of the cerebrovasculature intact. This approach will open a window for brain metastasis treatment that currently does not exist.

Key Points

1. TNFR1-selective TNF mutein induces selective permeabilization of brain metastases.
2. TNF mutein enables access across a therapeutically relevant size range (0.5-150 kDa).
3. TNF mutein shows low immunogenicity and toxicity supporting downstream clinical use.

Importance of the Study

Brain metastasis remains a major clinical challenge. In the early stages of tumor development, the blood-brain barrier (BBB) is intact, excluding ~98% of small molecule therapies and most antibodies. Earlier treatment of metastases has a greatly increased likelihood of success, and consequently, finding ways to circumvent the BBB is critical. We have generated a mutant human TNF protein (mutTNF) that is a highly selective agonist of the TNF type 1 receptor (TNFR1), and which induces selective permeabilization of the BBB at sites

of micrometastases in mouse models, while leaving the rest of the BBB intact. This mutTNF-induced permeabilization lasts for ≥24 hours, in line with typical drug half-lives, and enables access across a therapeutically relevant size range. The agent shows low potential immunogenicity and toxicity, supporting clinical use. This approach overcomes the hurdle of an intact BBB and opens a window of opportunity for brain metastases when they are otherwise invisible and untreatable.

Brain metastasis is a significant clinical problem, and the incidence is increasing. The blood-brain barrier (BBB) is a significant impediment to systemically administered therapies, particularly in the micrometastatic stages of tumor development when it is completely intact.¹ As systemic metastases are treated more effectively, it is becoming increasingly urgent to find ways to circumvent the BBB and enable earlier treatment of brain metastasis.^{1,2} A number of strategies have been developed to overcome the restrictions imposed by an intact BBB,³⁻⁹ but these all suffer one or more limitations, including transient windows of permeability (<1 hour), size-restricted access (<1 kDa), lack of targeting to tumor sites, dose-limiting toxicity, or a requirement for knowledge of tumor location.

We have previously shown that intravenous injection of tumor necrosis factor (TNF) induces BBB permeabilization selectively at sites of brain metastases.¹⁰ This selective permeabilization can be induced in the micrometastatic stage, when the BBB is intact, and leaves the rest of the cerebrovascular BBB unaffected.¹⁰ This approach yields a number of advantages over those discussed above, including an extended window (≥24 hours) of permeabilization, entry of agents across a therapeutically relevant size range (0.5-150 kDa), selective permeabilization only at metastatic sites, and the ability to target all metastatic tumors within the brain with no requirement for a priori knowledge of location.

While TNF is currently used in isolated limb perfusion for some cancers,^{11,12} dose-limiting off-target effects of systemically administered TNF prevent more widespread therapeutic use. Although we are already working below the maximum tolerated dose for TNF in humans,¹³ any

concerns about systemic toxicity could limit translation. Thus, a lower effective dose would be clinically advantageous. TNF binds to 2 primary receptors, TNF type 1 receptor (TNFR1) and TNF type 2 receptor (TNFR2). Although early clinical trials of TNF suggested that TNF-induced toxicity reflects TNFR2 activation in humans,¹⁴⁻¹⁶ later pre-clinical studies suggested that both TNF receptors may be involved.¹⁷⁻¹⁹

Our previous work suggested that the TNF-induced permeabilization is primarily mediated by endothelial TNFR1.¹⁰ With a view to clinical translation, therefore, the aim of this study was to develop a novel TNFR1-selective mutant of human TNF that enables selective permeabilization of the vasculature closely associated with brain micrometastases with higher affinity than current alternatives.^{20,21} With this approach, we aim to increase the efficiency of BBB permeabilization and reduce the dose required for permeabilization by eliminating binding to any other TNF receptors, thus minimizing the risk of toxicity.

Materials and Methods**Generation of Mutant TNF Variants With Selective Affinity for Human and Mouse TNFR1**

A panel of huTNF muteins (mutTNF) with high selectivity for human TNFR1 (huTNFR1) and mouse TNFR1 (mTNFR1) were generated by phage display based on a previously reported TNFR1-selective TNF mutein (huTNF_{R32W S86T}).^{20,21} Following selection against huTNFR1 and mTNFR1 and de-selection against human TNFR2 (huTNFR2), colonies were

screened for binding to huTNFR1, huTNFR2, and mTNFR1 by ELISA and tested for cellular cytotoxicity. The 10 most promising muteins were sequenced, expressed in *E. coli*, purified, and screened for binding to huTNFR1, mTNFR1, huTNFR2, and mouse TNFR2 (mTNFR2). Full details are available in the [Supplementary Information](#).

CD4⁺ T-Cell Epitope Avoidance

Protein sequences of the 10 lead mutTNFs were scanned using an in silico algorithm to identify predicted MHC (major histocompatibility complex) class II binding epitopes, using Proprietary iTope™ technology (Abzena, Cambridge, UK) and the TCED™ (Abzena, Cambridge, UK) of known protein sequence-related T-cell epitopes,²² with huTNF as the non-immunogenic reference.

Paracellular Permeability Assay in hCMEC/D3 Cells

Human brain microvascular endothelial hCMEC/D3 cells were cultured as described previously.²³ Permeabilizing activity of the 10 lead mutTNFs on monolayers of hCMEC/D3 cells was assessed using a FITC-labeled 70-kDa dextran tracer (Sigma-Aldrich, Dorset, UK) assay. Confluent monolayers on permeable polyester transwell inserts were treated with mutTNF, wild-type huTNF, or vehicle for 24 hours. Subsequently, paracellular flux of FITC-dextran across the insert was evaluated and permeability coefficients calculated, as described previously.^{24,25} Full details are available in the [Supplementary Information](#).

Mutein Half-Life in the Circulation

All animal experiments were approved by the University of Oxford Clinical Medicine Ethics Review Committee and the UK Home Office (Animals [Scientific Procedures] Act 1986) and conducted in accordance with the University of Oxford Policy on the Use of Animals in Scientific Research and the ARRIVE guidelines. Animals were injected intravenously with mutTNFs (1 µg in 100 µL saline) under isoflurane anesthesia, and blood was collected by cardiac puncture under terminal anesthesia at 0, 0.6, 2, 4, 6, 8, 30, and 60 minutes (n = 3 per time point/mutTNF) for ELISA measurement of mutTNF concentrations. Full details are available in the [Supplementary Information](#).

Dose-Response and Window of Permeabilization Studies in a Syngeneic Brain Metastasis Model

All animal experiments were approved as above and also conformed to the Guidelines for the Welfare and Use of Animals in Cancer Research.²⁶ For the in vivo experiments, metastatic mouse breast carcinoma 4T1-GFP cells were cultured as described previously.^{10,27} Female BALB/c mice (Charles River, Kent, UK) were anesthetized with isoflurane and injected via the left cardiac ventricle, under ultrasound guidance (Vevo 3100 Imaging System; Fujifilm

VisualSonics), with 1×10^5 4T1-GFP cells in 100 µL of sterile phosphate-buffered saline.^{10,27}

To determine the dose-response of permeabilization, mice were injected intravenously with 5, 16.7, 50, or 150 µg/kg of the most promising candidate mutTNF (G4) in 100 µL saline, or saline alone (n = 3-4 per group) at 13-day post-metastasis induction. This time point was chosen based on our previous data showing the onset of BBB breakdown at metastatic sites from days 13 to 14. Since our goal was to demonstrate de novo breakdown following mutein injection, we chose to use the latest possible time point before natural breakdown becomes significant, yielding the best balance between metastases that can be readily found histologically for analysis, but as little natural breakdown as possible. Mice were perfusion-fixed 2 hours later, and BBB permeability was assessed using either horseradish peroxidase (HRP) histochemistry or IgG immunohistochemistry; in the IgG cohort, the 150 µg/kg mutTNF dose was omitted owing to a lack of statistical significance between the 50 and 150 µg/kg doses in the HRP group. For HRP histochemistry, mice were injected intravenously with 100 µL type II HRP (300 units; Sigma-Aldrich, Dorset, UK) 30 minutes prior to transcardial perfusion-fixation with Karnovsky's fixative. For IgG assessment of BBB permeabilization, mice were transcardially perfusion-fixed with PLP_{light} fixative.

To determine the window of permeabilization, but still keeping the latest time point within the 13-day time frame, mice were injected via a tail vein with 50 µg/kg mutTNF G4 in 100 µL saline (n = 6), or saline only (n = 3), at day 10 and were perfusion-fixed 2, 12, 24, or 72 hours later for HRP histology. Full details of all in vivo experiments are available in the [Supplementary Information](#).

HRP and IgG Histochemistry to Assess BBB Permeability

For HRP histochemistry, alternate sections were stained with Hanker-Yates, as described previously,¹⁰ and cresyl violet (Sigma-Aldrich, Dorset, UK). Each metastasis >50 µm in diameter on cresyl violet sections was assigned as either positive or negative for HRP staining on the adjacent Hanker-Yates sections ([Supplementary Figure S1](#)). For IgG assessment of permeabilization, all brain sections were immunostained for IgG, and each metastasis counted as either positive or negative for IgG staining. Full details are available in the [Supplementary Information](#).

Magnetic Resonance Imaging (MRI) Assessment of BBB Permeability

BALB/c mice injected intracardially with 4T1-GFP cells underwent MRI 13 days after metastasis induction, as described previously.¹⁰ Pre- and post-Gd-DTPA T₁-weighted images were acquired before and 2 hours after mutTNF G4 injection (5, 16.7, or 50 µg/kg) or saline alone (n = 6 per group). Pre-Gd-DTPA images were subtracted from post-Gd-DTPA images and a mask was created for all voxels with signal intensity greater than mean ± 2SD

for normal brain. This mask was applied to the post-Gd images, which were then cross-referenced with the corresponding histological sections to confirm metastasis presence and percentage signal change in metastasis-containing regions of interests (ROIs) calculated. Full details of image acquisition and analysis are available in the [Supplementary Information](#).

Enhanced Delivery of the Clinical Antibody Therapy Trastuzumab

To determine whether mutTNF-induced BBB permeability increased delivery of a relevant clinical therapeutic, mice were injected intracardially with 4T1-GFP cells, as above. At day 13, mice were co-injected intravenously with trastuzumab (250 µg/kg) and either mutTNF G4 (50 µg/kg) or saline. Mice were transcardially perfusion-fixed with PLP_{light} 2 hours later. Brain sections were stained for human IgG to assess trastuzumab extravasation into metastases. Full details are available in the [Supplementary Information](#).

Assessment of Permeabilization in a Xenogeneic Brain Metastasis Model

To further test the efficacy of mutTNF G4, HER2-expressing human breast carcinoma cells, MDA231BR-HER2, were cultured in DMEM supplemented with 10% FCS and Zeocin™ Selection Reagent (Gibco) (300 µg/mL) to maintain HER2 expression. Cells were passaged at least once without Zeocin™, then 1×10^4 cells in 100 µL saline were injected into female SCID mice (Charles River, Kent, UK) via the left cardiac ventricle, as above.

Assessment of TNFR1 Expression in Additional Mouse Models of Brain Metastasis

TNFR1 expression was assessed in 3 xenogeneic brain metastasis models induced in SCID mice via intracardiac injection of 1×10^5 human breast cancer (MDA231Br-GFP), melanoma (H1_DL2), or lung cancer (SEBTA-001) cells, as described above and previously.²⁸ At day 21 (MDA231Br-GFP and H1_DL2) or day 28 (SEBTA-001), co-localization of TNFR1 and endothelial cells (CD31) was assessed immunofluorescently in the vicinity of metastases. Full details are available in the [Supplementary Information](#).

Toxicology Study

Animals were injected intravenously with 50 µg/kg of mTNF, huTNF or mutTNF (G4), or saline alone (n = 4 per group), and 24 hours later, blood was collected by cardiac puncture under isoflurane anesthesia. Blood samples were collected separately for hematology and clinical chemistry, and heart, lung, kidney, spleen, liver, and brain were removed from all animals. Samples were sent to MRC Harwell (Oxford, UK) for analysis. Full details are available in the [Supplementary Information](#).

Statistical Analysis

Statistical analysis was performed using Prism (GraphPad Software Inc.) and IBM SPSS 21 Statistics package (IBM Inc.). Shapiro-Wilk and Levene tests were applied to determine suitability for parametric or nonparametric tests. For BBB breakdown frequency (HRP and IgG), paracellular permeability, data were analyzed using a 1-way analysis of variance (ANOVA) followed by Tukey or Sidak post hoc test. Differences in the ratio of MRI signal intensity at metastatic sites vs equivalent regions in the contralateral hemisphere were assessed using a Kruskal-Wallis test, followed by uncorrected Dunn multiple comparison test. For toxicological analysis, parameters with parametric distributions were analyzed with 1-way ANOVA, followed by Dunnett post hoc test vs saline group. Nonparametric parameters were analyzed by Kruskal-Wallis test, followed by Dunn multiple comparison test. All statistical tests were 2-tailed. The frequency of positive and negative tumors for the small cohort study in the MDA231BR-HER2 model was laid out in a 2×2 contingency table for saline and mutTNF-treated animals and Fisher exact test was used to determine whether group memberships were different.

Results

Generation of mutTNF Variants With Selective Affinity for Human and Mouse TNFR1

From the panel of muTNFs generated, 10 top candidates were identified that all showed high-affinity binding for both huTNFR1 and mTNFR1 ([Figure 1A](#); [Supplementary Figure S2](#); [Supplementary Table S1](#)), and substantially higher affinity than the previously published huTNF_{R32W}^{S86T}; this recognized huTNFR1 with lower affinity than huTNF and did not recognize mTNFR1 ([Supplementary Figure S2](#)). One mutTNF in particular (G4; huTNF_{A84S, V85S, S86T, Q88N, T89P}) was identified as showing at least as high affinity for huTNFR1 as huTNF (8.72×10^{-12} vs 1.58×10^{-11} ; [Figure 1A](#); [Supplementary Table S1](#)). Although the affinity of the variant is apparently higher than that of huTNF, these measurements are at the limit of the sensitivity of the instrument. This mutTNF also showed comparable affinity for mTNFR1 as mTNF (1.40×10^{-10} vs 4.42×10^{-10}) and undetectable binding to both human and mouse TNFR2 (huTNFR2 and mTNFR2, respectively; [Figure 1A](#)), indicating selectivity for TNFR1.

Assessment of Immunogenicity

For clinical translation, minimizing immunogenicity is essential. For this reason, the protein sequences of our 10 lead muteins were scanned using an in silico algorithm to identify predicted MHC class II binding epitopes. While several mutTNFs exhibited both promiscuous high and moderate MHC class II-binding epitopes, G4 showed only one promiscuous moderate epitope ([Supplementary Table S2](#)) indicating a lower likelihood of immunogenicity.

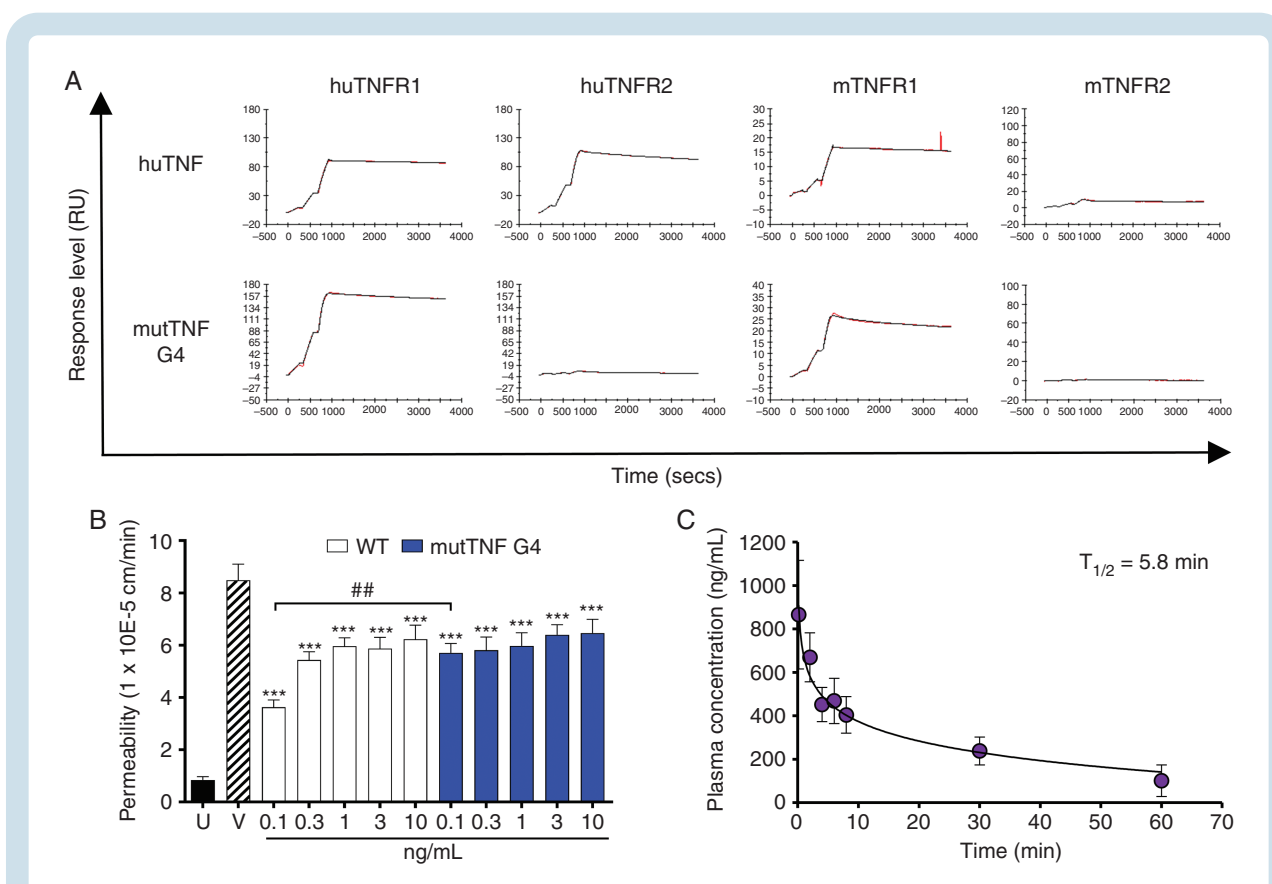


Fig. 1 Biological activity of mutTNF G4 in vitro. (A) Single-cycle kinetic sensorgram data (red lines) and fitted curves (black lines) for the binding of huTNF and mutTNF G4 to huTNFR1, huTNFR2, mTNFR1, and mTNFR2. (B) Assessment of alterations in permeability as reflected by changes in permeability coefficients (P_e) of a hCMEC/D3 cell monolayer treated with 0.1–10 ng/mL of huTNF (WT) or mutTNF (G4) for 24 hours, VEGF (V) as positive control, or untreated cells (U) as negative control. (C) Plasma concentrations (ng/mL) for mutTNF G4 at different time points after intravenous administration of 1 μ g. Statistical analysis: all values are expressed as mean \pm SD. 1-way ANOVA with Sidak post hoc test vs untreated group (***) $P < .005$ or huTNF group (##) $P < .01$. Abbreviations: mutTNF, TNF muteins; VEGF, vascular endothelial growth factor.

BBB Permeabilization of Endothelial Cell Monolayers

Permeabilizing efficacy of the mutTNFs was first assessed in vitro on a monolayer of immortalized human brain microvascular endothelial cells (hCMEC/D3). All mutTNFs induced significant permeability in vitro (Figure 1B; Supplementary Figure S3). However, mutTNF G4 showed a significantly higher permeability coefficient (P_e) than wild-type huTNF at the lowest dose studied (0.1 ng/mL; Figure 1B), indicating an enhanced permeabilizing activity.

Circulatory Half-Life

Four of the six mutTNFs tested exhibited a circulatory half-life similar to huTNF (5.6 minutes), including G4 (Figure 1C; Supplementary Figure S4). Since longer circulation is likely to lead to greater toxicity, a half-life close to that of huTNF is ideal as this will allow sufficient binding to its target to enable permeabilization, but minimize toxicity associated with longer circulation in the blood.

Taking all of the above data together, G4 was chosen as the most promising mutTNF and was, thus, taken forward into in vivo studies.

Dose-Response and Window of BBB Permeabilization

Initially, histological detection of HRP extravasation was used to assess in vivo BBB permeabilization induced by the mutTNF G4. HRP-positive metastases, indicating BBB breakdown, were evident in all mice treated with the mutTNF G4, with the number increasing in a dose-dependent manner (Figure 2). No breakdown was evident in non-tumor-bearing normal brain tissue. Some natural BBB breakdown was evident at metastatic sites in the saline group, as expected at this time point (day 13), particularly for brain metastases >400- μ m diameter. Nonetheless, the numbers of HRP-positive metastases as a percentage of total metastases ($47.8 \pm 3.3\%$, $55.1 \pm 8.0\%$, and $64.2 \pm 7.6\%$) at the 3 highest doses of mutTNF G4 (16.7, 50, and 150 μ g/kg, respectively) were

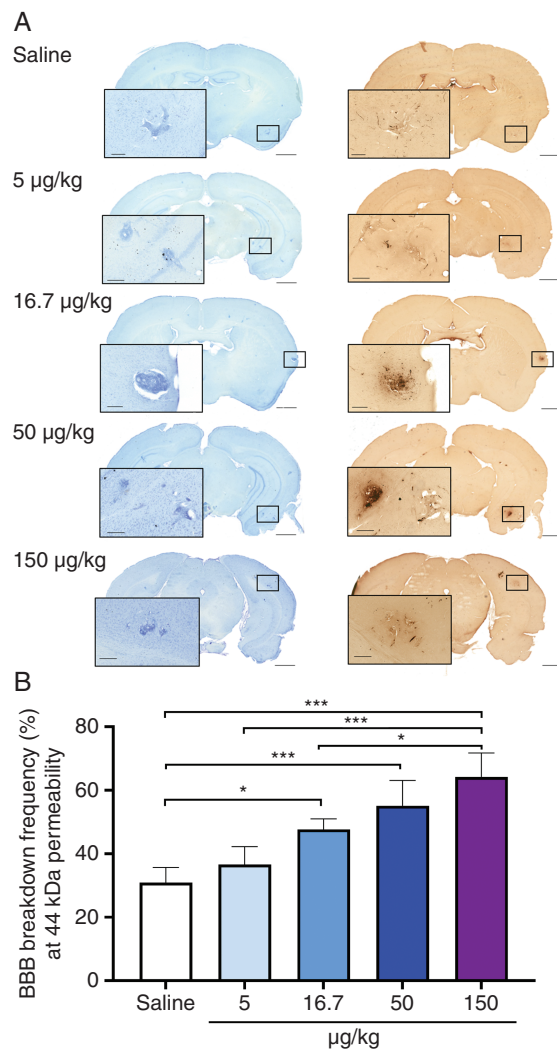


Fig. 2 Histological assessment of mutTNF-induced BBB breakdown by HRP histochemistry. (A) HRP (44 kDa) detection (brown) revealed areas of BBB breakdown at metastatic sites, as confirmed by cresyl violet histology on adjacent sections. (B) Graph showing dose-response analysis of metastasis-specific BBB breakdown frequency 2 hours after different doses of mutTNF ($n = 3/\text{group}$, except 50 µg/kg and saline where $n = 4$). Scale bars = 200 µm (enlarged inner square) and 1 mm. Statistical analysis: all values are expressed as mean \pm SD. 1-way ANOVA with post hoc Tukey test (* $P < .05$, *** $P < .005$). Abbreviations: BBB, blood-brain barrier; HRP, horseradish peroxidase; mutTNF, TNF muteins.

significantly greater than in the saline group ($30.9 \pm 4.8\%$; **Figure 2B**).

The above findings were confirmed by immunostaining for endogenous serum IgG, which is normally excluded from the brain by an intact BBB (**Figure 3A**). In this case, the percentages of IgG-positive metastases ($57.0 \pm 8.1\%$, $50.9 \pm 4.9\%$, and $41.2 \pm 1.4\%$; at 5, 16.7, and 50 µg/kg, respectively) were significantly greater than in the saline group ($26.6 \pm 2.3\%$) for all mutTNF doses (**Figure 3B**). Together,

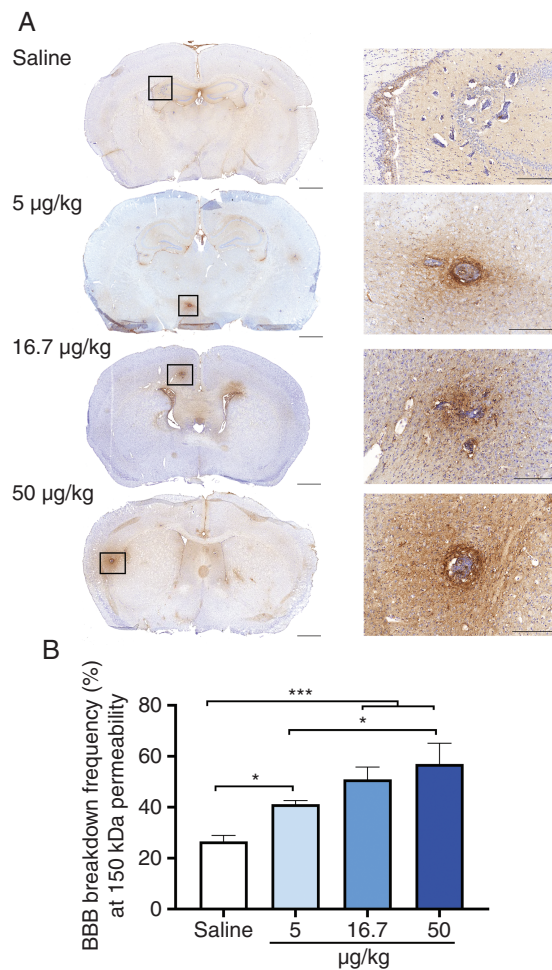
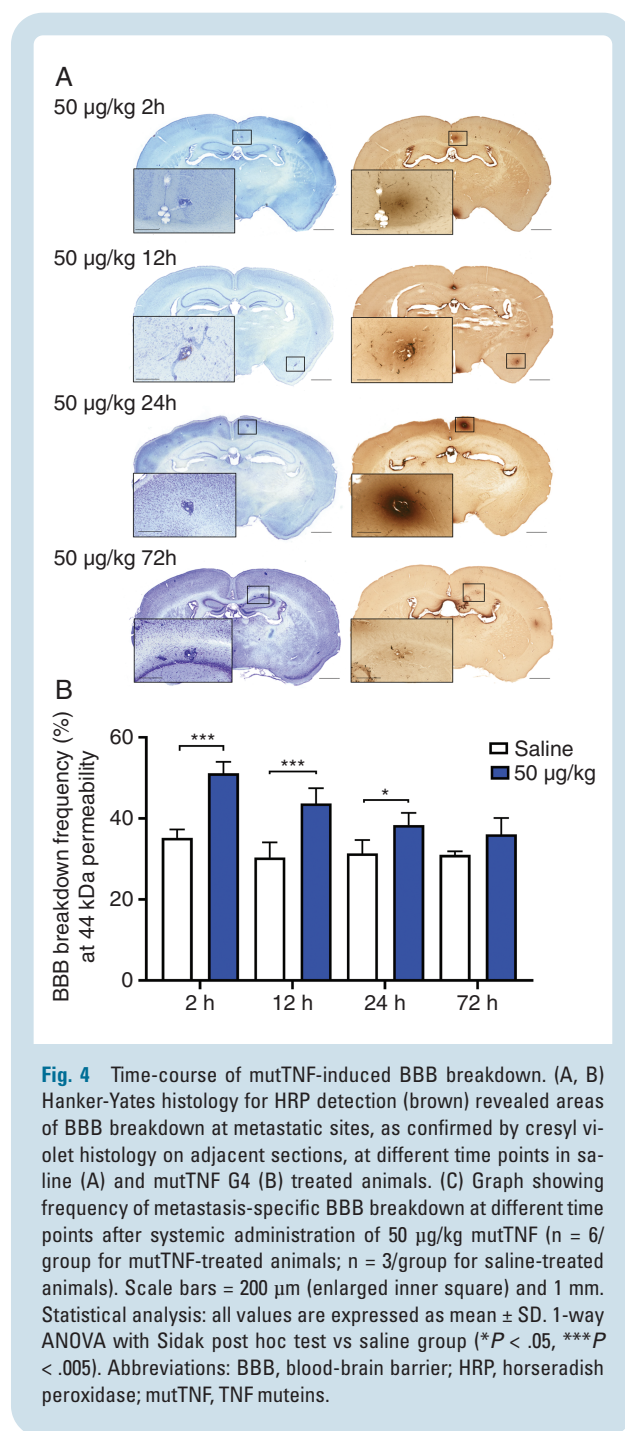


Fig. 3 Histological assessment of mutTNF-induced BBB breakdown by IgG immunostaining. (A) IgG (150 kDa) immunostaining (brown) revealed areas of BBB breakdown at metastatic sites; sections counterstained with cresyl violet. (B) Graph showing dose-response analysis of metastasis-specific BBB breakdown frequency 2 hours after different doses of mutTNF ($n = 3/\text{group}$). Scale bars = 200 µm (enlarged inner square) and 1 mm. Statistical analysis: all values are expressed as mean \pm SD. 1-way ANOVA with post hoc Tukey test (* $P < .05$, *** $P < .005$). Abbreviations: BBB, blood-brain barrier; mutTNF, TNF muteins.

these data indicate permeabilization across a size range spanning from 0.5 kDa (HRP) to 150 kDa (IgG), which would encompass the majority of, if not all, current therapeutics. Additional confocal immunofluorescent staining, for IgG and TNFR1 in mutTNF-treated animals, indicated close association between focal BBB breakdown at metastatic sites and endothelial TNFR1 upregulation (**Supplementary Figure S5**).

Next, the duration of BBB permeabilization induced by mutTNF administration (50 µg/kg) was assessed. Although BBB breakdown was evident at all time points after mutTNF administration, the percentage of HRP-positive metastases decreased over time (**Figure 4A**). Thus, significant breakdown was still evident in mutTNF



mice compared to saline-treated mice at 24-hour, but not 72-hour, posttreatment (Figure 4B). These results indicate that an extended window of permeabilization (≥ 24 hours) can be achieved with mutTNF administration.

Gd-DTPA Enhancement in Brain Metastases

To next assess BBB permeabilization in vivo, contrast-enhanced MRI was used. Extravasation and accumulation of Gd-DTPA enable BBB breakdown to be detected in vivo as hyperintense areas on T_1 -weighted MR images.

Post-Gd-DTPA T_1 -weighted images indicated a small number of metastases exhibiting natural BBB breakdown prior to mutTNF treatment, and these were excluded from the analysis.

At 2 hours after mutTNF treatment, areas of hyperintensity were evident on post-Gd-DTPA images compared to pre-Gd-DTPA images (Figure 5A–D), which corresponded spatially with sites of metastases (Figure 5E–F). Most animals in the saline group did not show Gd-DTPA contrast enhancement (Supplementary Figure S6A–C); where occasional hyperintensities were evident, these showed lower contrast and a more spatially restricted profile than in the mutTNF-treated animals (Supplementary Figure S6D–F). This low level of breakdown likely reflects natural breakdown at metastatic sites that were missed in the pretreatment scans owing to their lower resolution. The ratio of signal intensity at sites shown to contain metastases vs equivalent non-tumor-bearing regions was significantly greater at all mutTNF concentrations compared to the saline-injected group (Figure 5G).

Enhanced Delivery of the Clinically Used Antibody Therapy Trastuzumab

To assess whether mutTNF-induced BBB permeability increased delivery of a relevant therapeutic, 4T1-GFP metastasis bearing mice were injected concomitantly with trastuzumab and either mutTNF G4 or saline. As for the above HRP and IgG assessment of BBB breakdown, both positive and negative metastases for trastuzumab (human IgG) were evident in both groups (Figure 6). However, a significant increase in the number of trastuzumab positive metastases was evident in mice treated with mutTNF compared to control, saline-treated animals ($P < .01$; Figure 6). Moreover, where trastuzumab positivity was observed in the saline-treated animals, this tended to be of lower intensity than for mutTNF-treated animals (Figure 6A–D).

Permeabilization in a Xenogeneic Brain Metastasis Model

The permeabilizing action of mutTNF G4 was further assessed in a second brain metastasis model, MDA231BRHER2, by IgG immunostaining. Although only a small cohort of animals was studied, a significant increase in the percentage of IgG-positive metastases was evident in the mutTNF-treated animals (72.7%) compared to the saline group (14.3%); Fisher exact test indicated different group memberships for the 2 cohorts ($P < .05$; Supplementary Figure S7).

Assessment of TNFR1 Expression in Additional Mouse Models of Brain Metastasis

To evaluate the broader applicability of this approach, the expression of endothelial TNFR1 was assessed by confocal immunofluorescence microscopy in 3 further xenogeneic brain metastasis models; primary human breast cancer,

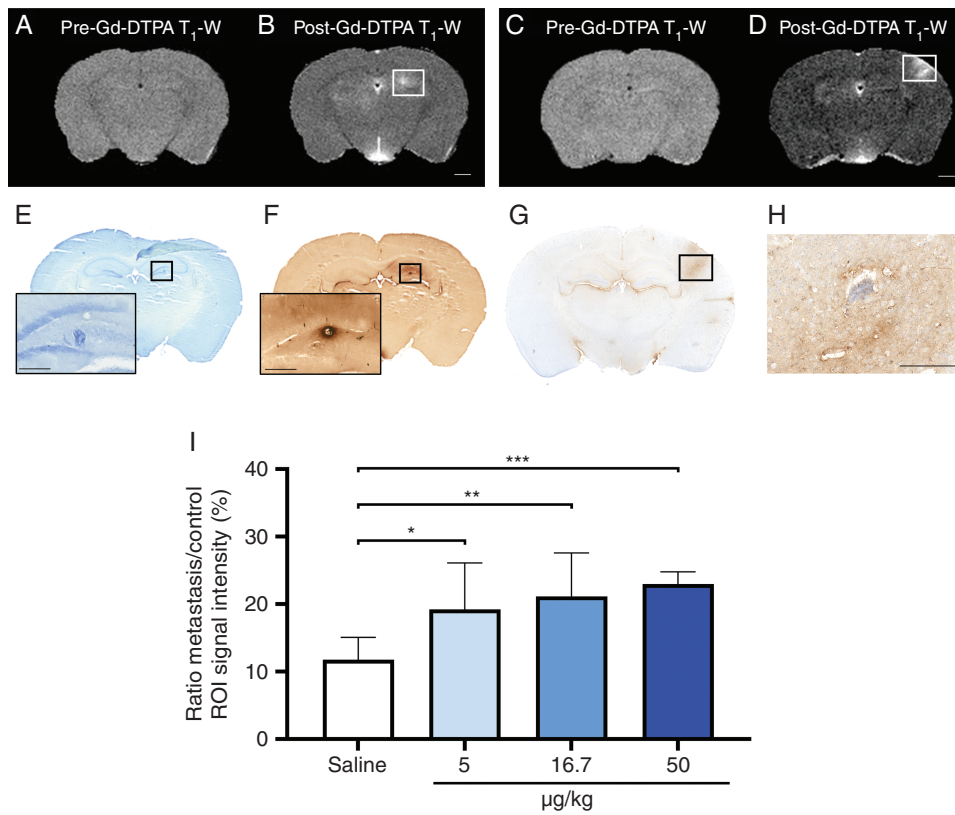


Figure 5. Gd-DTPA enhancement at metastatic sites. T₁-weighted images were acquired pre- (A, C) and 5-minute post-Gd-DTPA injection (B, D) 2 hours after systemic administration of 16.7 µg/kg (B) or 50 µg/kg (D) of mutTNF G4. Areas of high signal intensity (white) infer areas of BBB breakdown. The presence of metastasis within the white box in (B) was confirmed on a cresyl violet stained section (E) together with the adjacent Hanker-Yates section (F) confirming HRP extravasation (brown staining), and hence, BBB breakdown. (G) Histological confirmation of the presence of metastatic foci within the white box in (D) on a corresponding IgG-stained section; a metastasis is clearly visible at the center of the brown-stained region in the zoomed image of the boxed region in (H). Sections counterstained with cresyl violet. Scale bars = 200 µm (enlarged inner square) and 1 mm. (I) Graph showing percentage increase in signal intensity at metastatic sites (n = 6/group). Statistical analysis: all values are expressed as mean ± SD. Nonparametric Kruskal-Wallis test was performed with Dunn post hoc test vs saline group (**P* < .05, ***P* < .01, ****P* < .005). Abbreviations: BBB, blood-brain barrier; HRP, horseradish peroxidase.

melanoma, and lung cancer. In all cases, endothelialTNFR1 upregulation was clearly evident on tumor-surrounding vasculature (Supplementary Figure S8). No endothelial TNFR1 staining was found on normal appearing brain tissue.

Toxicological Assessment

Finally, single time point toxicological evaluation for mutTNF G4 was carried out at a dose of 50 µg/kg and compared to mTNF, huTNF, and saline as control; all evaluated 24 hours after administration. No pathological differences were evident in mutTNF injected mice compared to saline, huTNF, or mTNF for heart, lung, liver, brain, spleen, and kidney tissues at 2 days after administration. Similarly, no blood chemistry changes of concern were noted (Supplementary Table S3). Leucopenia was present in all 3 treatment groups (mutTNF, mTNF, and huTNF), but this is a known side effect of TNF, and

therefore, expected.²⁹ This leucopenia appeared to reflect a global reduction in all WBCs (Supplementary Table S4). No other hematological changes of concern were evident (Supplementary Table S4). Soluble mTNF levels in the blood were undetectable 24 hours after mutTNF G4 administration.

Discussion

Prognosis for patients with brain metastases is extremely poor, and studies suggest that earlier intervention is key to successful treatment. The presence of an intact BBB, which is characteristic during the early (micrometastasis) stages of tumor development, effectively excludes most systemic therapeutics and diagnostic imaging agents from tumor sites. In this study, we have developed a novel TNFR1-selective human TNF mutein (mutTNF), which has similar affinity for humanTNFR1 than huTNF, undetectable binding

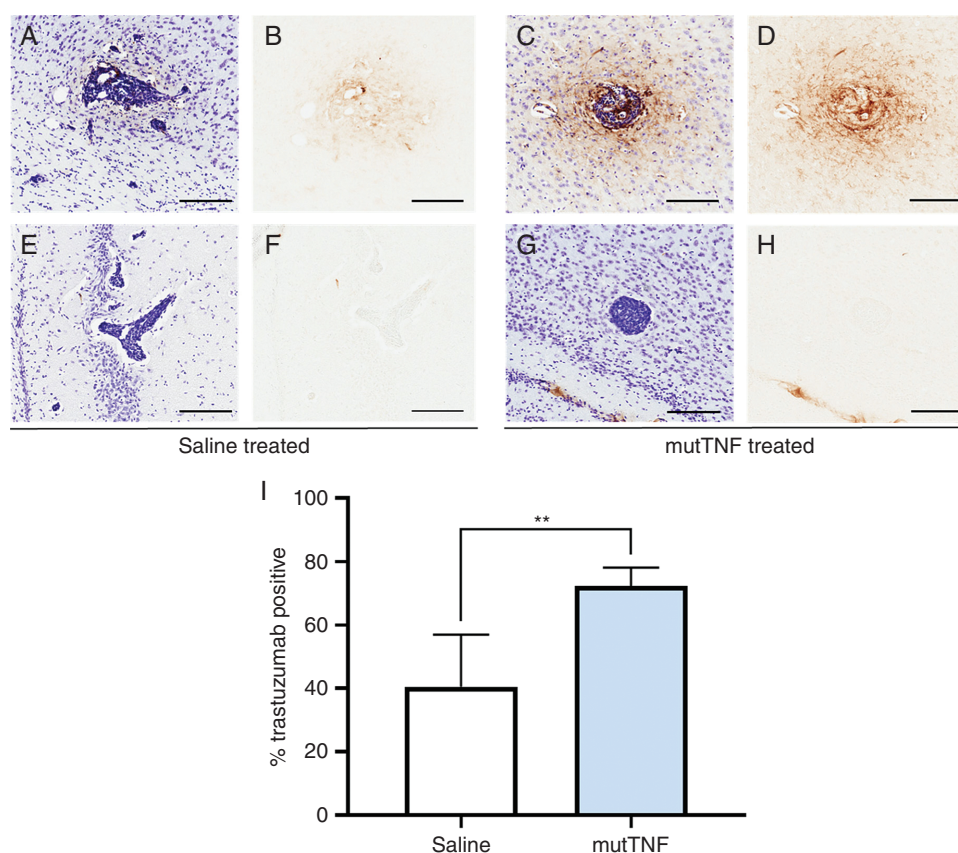


Figure 6. Trastuzumab extravasation after co-administration with either mutTNF or saline. (A–H) Example images of metastatic sites classified as either positive or negative for trastuzumab, as determined by human IgG immunostaining (brown). (A–D) Examples of IgG-positive metastases in a saline-treated mouse (A, B) and a mutTNF G4-treated mouse (C, D). (E–H) Examples of IgG negative metastases in a saline-treated mouse (E, F) and a mutTNF G4-treated mouse (G, H). Sections were first assessed for trastuzumab positivity (B, D, F, H; brown staining), and subsequently, counterstained with cresyl violet to verify the presence of metastases (A, C, G, E). Scale bars = 150 μ m. (I) Graph showing quantitative analysis of trastuzumab extravasation at sites of metastasis from saline control ($n = 3$ mice; $n = 714$ metastases) and mutTNF-treated ($n = 3$ mice; $n = 978$ metastases) groups; significantly greater extravasation of trastuzumab was evident in mutTNF-treated animals. Statistical analysis: all values are expressed as mean \pm SD. Nonparametric Mann-Whitney U test (** $P < .01$). Abbreviation: mutTNF, TNF muteins.

to human TNFR2, and induces permeabilization of a brain endothelial cell monolayer in vitro with higher sensitivity than huTNF. Subsequent in vivo studies, in 2 different mouse models, showed that intravenous injection of the mutTNF-induced BBB permeabilization selectively at sites of brain micrometastases. Permeabilization was observed for ≥ 24 hours and enabled the delivery of agents across a broad size range (0.5–150 kDa), including the clinically used therapeutic antibody trastuzumab. Upregulation of endothelial TNFR1 was found in xenogeneic models of brain metastasis from multiple different primary tumor origins (breast cancer, melanoma, and lung cancer), supporting the broad applicability and translational relevance of this approach. Finally, preliminary toxicology data, obtained 24 hours after administration, showed no contraindications to clinical translation.

A number of approaches to circumventing an intact BBB have been developed, but all suffer limitations. Kinin-mediated disruption of the BBB, while promising in preclinical studies,^{3,4,30} failed in early clinical trials

(eg, RMP-7) owing to dose-limiting side effects, size-restricted access (1 kDa), and short-lived (<1 hour) permeabilizing effects.⁹ Hyperosmotic opening of the BBB has progressed to Phase I trials,⁵ but has the significant disadvantage of permeabilizing the BBB globally and only confers very transient (<1 hour) permeability to agents of <1 kDa.^{6,31} Similarly, K16ApoE-mediated BBB permeabilization, although promising, results in global permeability and for only relatively short periods of time (ca. 1 hour).³² A similar idea based on receptor-mediated transcytosis using Fc fragments engineered to bind to the transferrin receptor (TfR) has also been described.³³ However, there is no evidence that endothelial cells associated with brain metastases express more TfR than endothelial cells in normal brain, which is critical to obtaining selective BBB opening. Drugs modified to enhance crossing of the BBB (eg, liposomally packaged doxorubicin) have progressed to early phase clinical trials.^{7,34} However, a combination of such agents with focused ultrasound (FUS)-mediated BBB disruption has been necessary to achieve the most

effective outcomes,^{8,35} requiring prior knowledge of tumor location. This approach, therefore, will not enable brain metastases to be treated at the micrometastatic stage when they are currently undetectable. Similarly, targeting of angiogenic tumor vasculature specifically, either via $\alpha_v\beta_3$ -targeted phage mediated drug delivery³⁶ or CD13-targeted TNF-induced permeabilization,³⁷ focusses on later stage tumors and is less applicable in the early micrometastatic stages when angiogenesis is limited. Finally, although circumventing the BBB is a major barrier to drug access, tumor interstitial fluid pressure (IFP) can also be a significant impediment³⁸ and thus, combining approaches that target the BBB together with those that alleviate tumor IFP (eg, dexamethasone, extracellular matrix targeting peptides)^{39,40} may prove most effective particularly for larger tumors. Interestingly, FUS-induced BBB disruption has recently been shown to both increase drug extravasation and enhance interstitial convective transport in brain tumors, thus apparently overcoming both the BBB and tumor IFP.⁴¹ However, as noted above, FUS relies on knowledge of tumor location and is, therefore, more relevant to the treatment of later-stage macrometastases. Moreover, early-stage micrometastases, which are growing co-optimally along vessels, do not yet exhibit many of the features leading to raised tumor IFP, and consequently, overcoming the intact BBB remains the greatest challenge.

TNF has 2 isoforms, which are able to activate both TNFR1 and TNFR2. Activation of TNFR1 alone can induce a range of responses from cell survival to apoptosis, necroptosis, and necrosis.⁴² Nevertheless, the exact mechanisms of TNF-induced toxicity, and the relative importance of the 2 receptors, remain unclear. Early clinical trials of TNF showed a disappointingly high level of adverse effects, and with the finding that huTNF is an agonist of mTNFR1 only,^{14,15} suggested that TNF-induced toxicity in humans reflects TNFR2 activation. Subsequent studies in mice showed that TNFR2 overexpression sensitizes mice to a sublethal dose of TNF,¹⁶ while a mutant mTNF with 50-fold lower TNFR2-mediated bioactivity showed significantly reduced toxicity compared to mTNF.⁴³ Finally, studies in mice have shown that a TNFR1-targeted mutein is nontoxic well above the maximum tolerated dose of mTNF.¹⁵ Other studies, however, have demonstrated some systemic toxicity in baboons injected with a TNFR1-specific mutein,⁴⁴ while work with either TNFR1 knockout mice,¹⁷ or downregulation of TNFR1 with antisense oligonucleotides,¹⁸ have demonstrated reduced systemic toxicity to mTNF. Moreover, while a number of studies suggest that activation of TNFR2 can induce toxicity directly,^{45,46} others suggest an indirect mechanism ("ligand-passing") whereby the local TNF concentration around TNFR1 is effectively increased.¹⁹ Together, these findings suggest that both TNF receptors contribute to the systemic toxicity of TNF.

Here, we propose that by targeting a single TNF receptor toxicity can be reduced, firstly, by eliminating toxicity associated with binding to one subset of receptors, and secondly, by lowering the required permeabilization dose as none is lost through off-target binding. Based on our previous work, indicating that TNF-induced permeabilization in brain metastases was

primarily TNFR1-mediated,¹⁰ our aim was to develop a TNFR1-selective mutant of human TNF, that induces permeabilization selectively at sites of brain metastases and could be used clinically. While other huTNFR1-selective agonists have been developed previously, these have either shown low affinity for mTNFR1, precluding their use in animal models and reducing the relevance of pre-clinical toxicology, or they have shown lower binding affinity to huTNFR1 than huTNF and/or residual affinity to TNFR2.^{20,47} In contrast, our novel TNFR1-selective mutTNF has an order of magnitude higher affinity for huTNFR1 than huTNF and undetectable binding to huTNFR2. In addition, this mutTNF has similar affinity for mTNFR1 as mTNF enabling in vivo testing and meaningful downstream toxicology.

Importantly, this mutTNF-induced permeabilization in a mouse model of brain metastasis across a size range spanning from 0.5 kDa (HRP) to 150 kDa (IgG), which would encompass the majority of, if not all, current therapeutics in terms of size. While there may be differences in hydrophobicity, charge, and molecular structure of different therapeutics, the delivery of a range of molecules in the current study (HRP, Gd-DTPA, and IgG), which exhibit significant differences in such properties, suggests that the permeability induced by mutTNF administration could facilitate delivery of many therapeutics. This is particularly pertinent for monoclonal antibody-based therapies such as trastuzumab (145.5 kDa), pertuzumab (137.9 kDa), and durvalumab (149 kDa), which have shown considerable promise in metastatic cancer but are unable to cross the intact BBB. In accord with this notion, we subsequently demonstrated that co-administration of mutTNF and trastuzumab does significantly enhance the delivery of this antibody to micrometastatic sites in the brain.

One concern for the use of mutTNF is whether it may lead to the development of more invasive brain metastases, as has been suggested for TNF whereby its vascular effects drive epithelial-to-mesenchymal (EMT) transition.⁴⁸ We have demonstrated, however, that the mutein did not lead to induction of endogenous TNF production, which would be essential for driving EMT transition.⁴⁹ Moreover, we have previously shown that direct injection of TNF into the brain does not induce endogenous TNF production within the brain itself.⁵⁰ Finally, measurement of tumor volumes in the cohort of animals that were evaluated 72 hours after single dose of mutTNF showed no significant differences in tumor volumes between the control and mutTNF-treated animals (Supplementary Figure S9). These findings do not exclude the possibility that multiple doses of mutTNF may lead to effects on tumor invasiveness. However, the mutTNF would only be administered in combination with a therapeutic agent, which would be expected to mitigate against any such effects.

A further potential issue is that in this work, a single dose of mutTNF did not appear to induce BBB breakdown in all metastatic foci. This apparent lack of response in some metastases could reflect sensitivity limitations of the histological approaches used, and/or the fact that some metastases induce lower levels of endothelial TNFR1 resulting in a response that is below the detection limits of the method. In practice, we anticipate that repeated doses are likely in a

clinical setting, in line with treatment regimes, and that this would counteract any lower responses.

In conclusion, this work shows the development of a novel, clinically translatable TNFR1-selective agent that is able to induce transient BBB breakdown at sites of micrometastases where it would otherwise be completely intact. In comparison to other strategies for permeabilizing the BBB, this approach yields an extended window (≥ 24 hours) of permeabilization, in keeping with typical half-lives of therapeutics, and facilitates permeability across a therapeutically relevant size range with no requirement for drug modification. Permeabilization is induced selectively at metastatic sites and all metastatic tumors within the brain are targeted, including micrometastases that are currently undetectable, with no knowledge of location required. Finally, upregulation of the endothelial target TNFR1 has been demonstrated across multiple models of brain metastasis, from different primary tumor types, indicating the broad applicability of this approach. Thus, the combination of this agent with systemic therapeutics will enable significantly earlier treatment of brain metastases, at a time when curative potential is greatest.

Supplementary Material

Supplementary material is available at *Neuro-Oncology* online.

Keywords

blood-brain barrier | brain metastasis | mutein | permeabilization | tumor necrosis factor

Funding

This work was supported by the Medical Research Council (MR/N028031/1), Cancer Research UK (C5255/A15935), and the CRUK/EPSRC Cancer Imaging Centre in Oxford (C5255/A16466).

Acknowledgments

The authors thank members of the BMS staff and Imaging Core within the Institute for Radiation Oncology for core support with animal husbandry and MRI, respectively, and Prof. Ignacio Romero (Open University, UK) for the kind gift of the hCMEC/D3 cells.

Conflict of interest statement. The work in this manuscript is the subject of a patent application, currently pending. N.R.S., D.C.A., and S.J.C. are inventors on this patent, and M.F.M.P. is a contributor.

Authorship statement. N.R.S. and D.C.A. conceived the project. N.R.S., D.C.A., S.J.C., and M.F.M.P. designed the experiments. M.F.M.P., V.A.J., C.B., V.W.T.C., N.Z., J.R.L., C.S.K., M.P., A.H., C.C., B.B.N., E.B., and R.H. obtained and analyzed the data. M.F.M.P. and N.R.S. wrote the manuscript. All authors revised the manuscript.

References

1. Eichler AF, Chung E, Kodack DP, Loeffler JS, Fukumura D, Jain RK. The biology of brain metastases-translation to new therapies. *Nat Rev Clin Oncol*. 2011;8(6):344–356.
2. Hersh DS, Wadajkar AS, Roberts N, et al. Evolving drug delivery strategies to overcome the blood brain barrier. *Curr Pharm Des*. 2016;22(9):1177–1193.
3. Côté J, Bovenzi V, Savard M, et al. Induction of selective blood-tumor barrier permeability and macromolecular transport by a biostable kinin B1 receptor agonist in a glioma rat model. *PLoS One*. 2012;7(5):e37485.
4. Côté J, Savard M, Neugebauer W, Fortin D, Lepage M, Gobeil F. Dual kinin B1 and B2 receptor activation provides enhanced blood-brain barrier permeability and anticancer drug delivery into brain tumors. *Cancer Biol Ther*. 2013;14(9):806–811.
5. Guillaume DJ, Doolittle ND, Gahramanov S, Hedrick NA, Delashaw JB, Neuwelt EA. Intra-arterial chemotherapy with osmotic blood-brain barrier disruption for aggressive oligodendroglial tumors: results of a phase I study. *Neurosurgery*. 2010;66(1):48–58; discussion 58.
6. Ikeda M, Nagashima T, Bhattacharjee AK, Kondoh T, Kohmura E, Tamaki N. Quantitative analysis of hyperosmotic and hypothermic blood-brain barrier opening. In: Kuroiwa T, Baethmann A, Czernicki Z, et al., eds. *BT - Brain Edema XII*. Vienna: Springer; 2003:559–563.
7. Caraglia M, Addeo R, Costanzo R, et al. Phase II study of temozolomide plus pegylated liposomal doxorubicin in the treatment of brain metastases from solid tumours. *Cancer Chemother Pharmacol*. 2006;57(1):34–39.
8. Mainprize T, Lipsman N, Huang Y, et al. Blood-brain barrier opening in primary brain tumors with non-invasive MR-guided focused ultrasound: a clinical safety and feasibility study. *Sci Rep*. 2019;9(1):321.
9. Prados MD, Schold SC Jr, Fine HA, et al. A randomized, double-blind, placebo-controlled, phase 2 study of RMP-7 in combination with carboplatin administered intravenously for the treatment of recurrent malignant glioma. *Neuro Oncol*. 2003;5(2):96–103.
10. Connell JJ, Chatain G, Cornelissen B, et al. Selective permeabilization of the blood-brain barrier at sites of metastasis. *J Natl Cancer Inst*. 2013;105(21):1634–1643.
11. Lejeune FJ, Liénard D, Matter M, Rüegg C. Efficiency of recombinant human TNF in human cancer therapy. *Cancer Immun*. 2006;6:6.
12. Eggermont AM, Schraffordt Koops H, Liénard D, et al. Isolated limb perfusion with high-dose tumor necrosis factor-alpha in combination with interferon-gamma and melphalan for nonresectable extremity soft tissue sarcomas: a multicenter trial. *J Clin Oncol*. 1996;14(10):2653–2665.
13. Terlikowski SJ. Local immunotherapy with rhTNF-alpha mutein induces strong antitumor activity without overt toxicity – a review. *Toxicology*. 2002;174(3):143–152.
14. Lewis M, Tartaglia LA, Lee A, et al. Cloning and expression of cDNAs for two distinct murine tumor necrosis factor receptors demonstrate one receptor is species specific. *Proc Natl Acad Sci USA*. 1991;88(7):2830–2834.

15. Kumaratilake LM, Rathjen DA, Mack P, Widmer F, Prasertsiriroj V, Ferrante A. A synthetic tumor necrosis factor- α agonist peptide enhances human polymorphonuclear leukocyte-mediated killing of *Plasmodium falciparum* in vitro and suppresses *Plasmodium chabaudi* infection in mice. *J Clin Invest*. 1995;95(5):2315–2323.
16. Douni E, Kollias G. A critical role of the p75 tumor necrosis factor receptor (p75TNF-R) in organ inflammation independent of TNF, lymphotoxin α , or the p55TNF-R. *J Exp Med*. 1998;188(7):1343–1352.
17. Van Hauwermeiren F, Armaka M, Karagianni N, et al. Safe TNF-based antitumor therapy following p55TNFR reduction in intestinal epithelium. *J Clin Invest*. 2013;123(6):2590–2603.
18. Van Hauwermeiren F, Vandenbroucke RE, Grine L, et al. Antisense oligonucleotides against TNFR1 prevent toxicity of TNF/IFN γ treatment in mouse tumor models. *Int J Cancer*. 2014;135(3):742–750.
19. Siegmund D, Kums J, Ehrenschrwender M, Wajant H. Activation of TNFR2 sensitizes macrophages for TNFR1-mediated necroptosis. *Cell Death Dis*. 2016;7(9):e2375.
20. Loetscher H, Stueber D, Banner D, Mackay F, Lesslauer W. Human tumor necrosis factor α (TNF α) mutants with exclusive specificity for the 55-kDa or 75-kDa TNF receptors. *J Biol Chem*. 1993;268(35):26350–26357.
21. Shibata H, Yoshioka Y, Ohkawa A, et al. Creation and X-ray structure analysis of the tumor necrosis factor receptor-1-selective mutant of a tumor necrosis factor- α antagonist. *J Biol Chem*. 2008;283(2):998–1007.
22. Bryson CJ, Jones TD, Baker MP. Prediction of immunogenicity of therapeutic proteins: validity of computational tools. *BioDrugs*. 2010;24(1):1–8.
23. Lopez-Ramirez MA, Fischer R, Torres-Badillo CC, et al. Role of caspases in cytokine-induced barrier breakdown in human brain endothelial cells. *J Immunol*. 2012;189(6):3130–3139.
24. Weksler B, Romero IA, Couraud PO. The hCMEC/D3 cell line as a model of the human blood brain barrier. *Fluids Barriers CNS*. 2013;10(1):16.
25. Helms HC, Abbott NJ, Burek M, et al. In vitro models of the blood-brain barrier: an overview of commonly used brain endothelial cell culture models and guidelines for their use. *J Cereb Blood Flow Metab*. 2016;36(5):862–890.
26. Workman P, Aboagye EO, Balkwill F, et al.; Committee of the National Cancer Research Institute. Guidelines for the welfare and use of animals in cancer research. *Br J Cancer*. 2010;102(11):1555–1577.
27. Serres S, Soto MS, Hamilton A, et al. Molecular MRI enables early and sensitive detection of brain metastases. *Proc Natl Acad Sci USA*. 2012;109(17):6674–6679.
28. Cheng VWT, Soto MS, Khrapitchev AA, et al. VCAM-1-targeted MRI enables detection of brain micrometastases from different primary tumors. *Clin Cancer Res*. 2019;25(2):533–543.
29. Aggarwal S, Gollapudi S, Gupta S. Increased TNF- α -induced apoptosis in lymphocytes from aged humans: changes in TNF- α receptor expression and activation of caspases. *J Immunol*. 1999;162(4):2154–2161.
30. Kuhr F, Lowry J, Zhang Y, Brovkovich V, Skidgel RA. Differential regulation of inducible and endothelial nitric oxide synthase by kinin B1 and B2 receptors. *Neuropeptides*. 2010;44(2):145–154.
31. Rapoport SI. Advances in osmotic opening of the blood-brain barrier to enhance CNS chemotherapy. *Expert Opin Investig Drugs*. 2001;10(10):1809–1818.
32. Aasen SN, Espedal H, Holte CF, et al. Improved drug delivery to brain metastases by peptide-mediated permeabilization of the blood-brain barrier. *Mol Cancer Ther*. 2019;18(11):2171–2181.
33. Kariolis MS, Wells RC, Getz JA, et al. Brain delivery of therapeutic proteins using an Fc fragment blood-brain barrier transport vehicle in mice and monkeys. *Sci Transl Med*. 2020;12(545):eaay1359.
34. Chastagner P, Devicor B, Geoerger B, et al. Phase I study of non-pegylated liposomal doxorubicin in children with recurrent/refractory high-grade glioma. *Cancer Chemother Pharmacol*. 2015;76(2):425–432.
35. Aryal M, Vykhodtseva N, Zhang YZ, McDannold N. Multiple sessions of liposomal doxorubicin delivery via focused ultrasound mediated blood-brain barrier disruption: a safety study. *J Control Release*. 2015;204:60–69.
36. Przystal JM, Waramit S, Pranjol MZI, et al. Efficacy of systemic temozolomide-activated phage-targeted gene therapy in human glioblastoma. *EMBO Mol Med*. 2019;11(4):e8492.
37. Gregor V, Citterio G, Vitali G, et al. Defining the optimal biological dose of NGR-hTNF, a selective vascular targeting agent, in advanced solid tumours. *Eur J Cancer*. 2010;46(1):198–206.
38. Stylianopoulos T, Munn LL, Jain RK. Reengineering the physical microenvironment of tumors to improve drug delivery and efficacy: from mathematical modeling to bench to bedside. *Trends Cancer*. 2018;4(4):292–319.
39. Navalitloha Y, Schwartz ES, Groothuis EN, Allen CV, Levy RM, Groothuis DR. Therapeutic implications of tumor interstitial fluid pressure in subcutaneous RG-2 tumors. *Neuro Oncol*. 2006;8(3):227–233.
40. Kang T, Zhu Q, Jiang D, et al. Synergistic targeting tenascin C and neuropilin-1 for specific penetration of nanoparticles for anti-glioblastoma treatment. *Biomaterials*. 2016;101:60–75.
41. Arvanitis CD, Askoxylakis V, Guo Y, et al. Mechanisms of enhanced drug delivery in brain metastases with focused ultrasound-induced blood–tumor barrier disruption. *Proc Natl Acad Sci USA*. 2018;115(37):E8717–E8726.
42. Wajant H, Siegmund D. TNFR1 and TNFR2 in the control of the life and death balance of macrophages. *Front Cell Dev Biol*. 2019;7:91.
43. Lucas R, Echtenacher B, Sablon E, et al. Generation of a mouse tumor necrosis factor mutant with antiperitonitis and desensitization activities comparable to those of the wild type but with reduced systemic toxicity. *Infect Immun*. 1997;65(6):2006–2010.
44. Van Zee KJ, Stackpole SA, Montegut WJ, et al. A human tumor necrosis factor (TNF) α mutant that binds exclusively to the p55 TNF receptor produces toxicity in the baboon. *J Exp Med*. 1994;179(4):1185–1191.
45. Kumar S, Joos G, Boon L, Tournoy K, Provost S, Maes T. Role of tumor necrosis factor- α and its receptors in diesel exhaust particle-induced pulmonary inflammation. *Sci Rep*. 2017;7(1):11508.
46. Depuydt B, van Loo G, Vandenabeele P, Declercq W. Induction of apoptosis by TNF receptor 2 in a T-cell hybridoma is FADD dependent and blocked by caspase-8 inhibitors. *J Cell Sci*. 2005;118(Pt 3):497–504.
47. Van Ostade X, Vandenabeele P, Everaerd B, et al. Human TNF mutants with selective activity on the p55 receptor. *Nature*. 1993;361(6409):266–269.
48. Cruceriu D, Baldasici O, Balacescu O, Berindan-Neagoe I. The dual role of tumor necrosis factor- α (TNF- α) in breast cancer: molecular insights and therapeutic approaches. *Cell Oncol (Dordr)*. 2020;43(1):1–18.
49. Bates RC, Mercurio AM. Tumor necrosis factor- α stimulates the epithelial-to-mesenchymal transition of human colonic organoids. *Mol Biol Cell*. 2003;14(5):1790–1800.
50. Blond D, Campbell SJ, Butchart AG, Perry VH, Anthony DC. Differential induction of interleukin-1 β and tumour necrosis factor- α may account for specific patterns of leukocyte recruitment in the brain. *Brain Res*. 2002;958(1):89–99.